

# Demixing of active particles in the presence of external fields

Sunita Kumari,<sup>1</sup> André S. Nunes,<sup>1</sup> Nuno A. M. Araujo,<sup>1,\*</sup> and Margarida M. Telo da Gama<sup>1</sup>

<sup>1</sup>*Departamento de Física, Faculdade de Ciências, Universidade de Lisboa,  
P-1749-016 Lisboa, Portugal and Centro de Física Teórica e Computacional,  
Universidade de Lisboa, P-1749-016, Lisboa, Portugal*

Active systems are inherently out of equilibrium, as they collect energy from their surroundings and transform it into directed motion. A recent theoretical study suggests that binary mixtures of active particles with distinct effective diffusion coefficients exhibit dynamical demixing above a threshold ratio of the diffusion coefficients. Here, we show that this threshold may be reduced drastically in the presence of external fields. We investigate the demixing as a function of the ratio of the diffusion coefficients and discuss the implications of the results for active systems.

## I. INTRODUCTION

Multicomponent systems may demix dynamic when the response of distinct species to external fields differ significantly [1–10]. Typical examples are mixtures of colloidal particles with different electrophoretic mobilities in the presence of an external field [4, 7] or granular mixtures of particles with different masses on vibrating plates [8, 11]. However, dynamical demixing does not necessarily require an external field. In active systems, demixing has been observed for mixtures of particles with significantly different activities [12] or effective diffusion coefficients [13].

Active particles are self-propelled random walkers that collect energy from their surroundings and convert it into propelled motion [14]. This constant flow of energy, drives active particles away from thermodynamic equilibrium leading to interesting new features that drive several active lines of research [15]. One of the simplest theoretical models for the dynamics of active particles consists of two-dimensional Brownian motion with translational diffusion coefficient  $D_T$ , and an additional propulsion force of strength  $v$ , along a preferred direction. This direction is coupled to the rotational degrees of freedom and evolves in time as a Brownian process with rotational diffusion coefficient  $D_R$ . The overall dynamics will depend on the ratios of these values. While at very short times, the motion is ballistic along the preferred direction, at significantly long times, Brownian dynamics is observed with an effective translational diffusion coefficient  $D_{\text{eff}} = D_T + \frac{1}{2}v^2/D_R$  [15].

Living active systems often consist of mixtures of passive and active particles or species with different activities [12, 16–26]. Recently, Weber *et al.* investigated the dynamics of binary mixtures of active particles with different diffusion coefficients and the same Stokes coefficient (mobility) [13]. They considered two species with diffusion coefficients  $D_L$  and  $D_H$ , respectively, with  $D_H \geq D_L$ . They found that, at sufficiently low  $D = D_L/D_H$ , the system demixes dynamically, forming solid-like clusters of slow diffusing particles surrounded by a

gas of rapidly diffusing ones. For a packing fraction of 0.5, demixing occurs at  $D \lesssim 10^{-2}$  and this threshold decreases as the packing fraction decreases.

In what follows, we discuss the possibility of using external fields to promote dynamical demixing. External stimuli (e.g., chemical/thermal gradients and electromagnetic fields) modify the particles trajectories, through the creation of distinct regions that localize one or both species [27–32]. For simplicity, we consider periodic (sinusoidal) potentials and identical responses to external field, i.e., identical electrophoretic mobilities in external electromagnetic fields. The results of the Brownian dynamics simulations, reported below, reveal that as the amplitude of the external potential increases the threshold value of  $D$  increases. Also, the solid-like cluster of slow diffusing particles is always localized along the minimum of the potential.

The paper is organized as follows. The description of the model and the simulations are presented in the next Section. We report and discuss the results in Sec. III. Finally, we draw some conclusions in Sec. IV.

## II. MODEL AND SIMULATION

As in Ref. [13], we consider a two-dimensional binary mixture of  $N$  particles (disks).  $N_H = N/2$  particles are of species H and the other  $N_L = N/2$  are of species L, corresponding to different effective diffusion coefficients  $D_H$  and  $D_L$ , respectively, where  $D_H \geq D_L$ . Particles move in a square box of linear dimension  $L_b$  with periodic boundary conditions in both directions. Since we are interested in timescales that are much larger than the Stokes time, we will consider that all particles are in the overdamped regime. Accordingly, the stochastic trajectory of particle  $i$  is obtained by solving the equation,

$$\dot{\vec{r}}_i = \vec{\eta}_i(t) + \mu \sum_{j=1}^N \vec{F}_{ij}(t) - \nabla_{\vec{r}_i} V_{\text{ext}}(\vec{r}_i), \quad (1)$$

where  $\vec{r}_i$  is the position of the particle. Particle interactions are given by short-ranged repulsive forces,  $\vec{F}_{ij} = \alpha(2a - r_{ij})\hat{r}_{ij}$ , accounting for particle overlap ( $r_{ij} < 2a$ ), where  $a$  is the particle radius, and vanishing  $\vec{F}_{ij} = 0$ ,

\* nmaraujo@fc.ul.pt

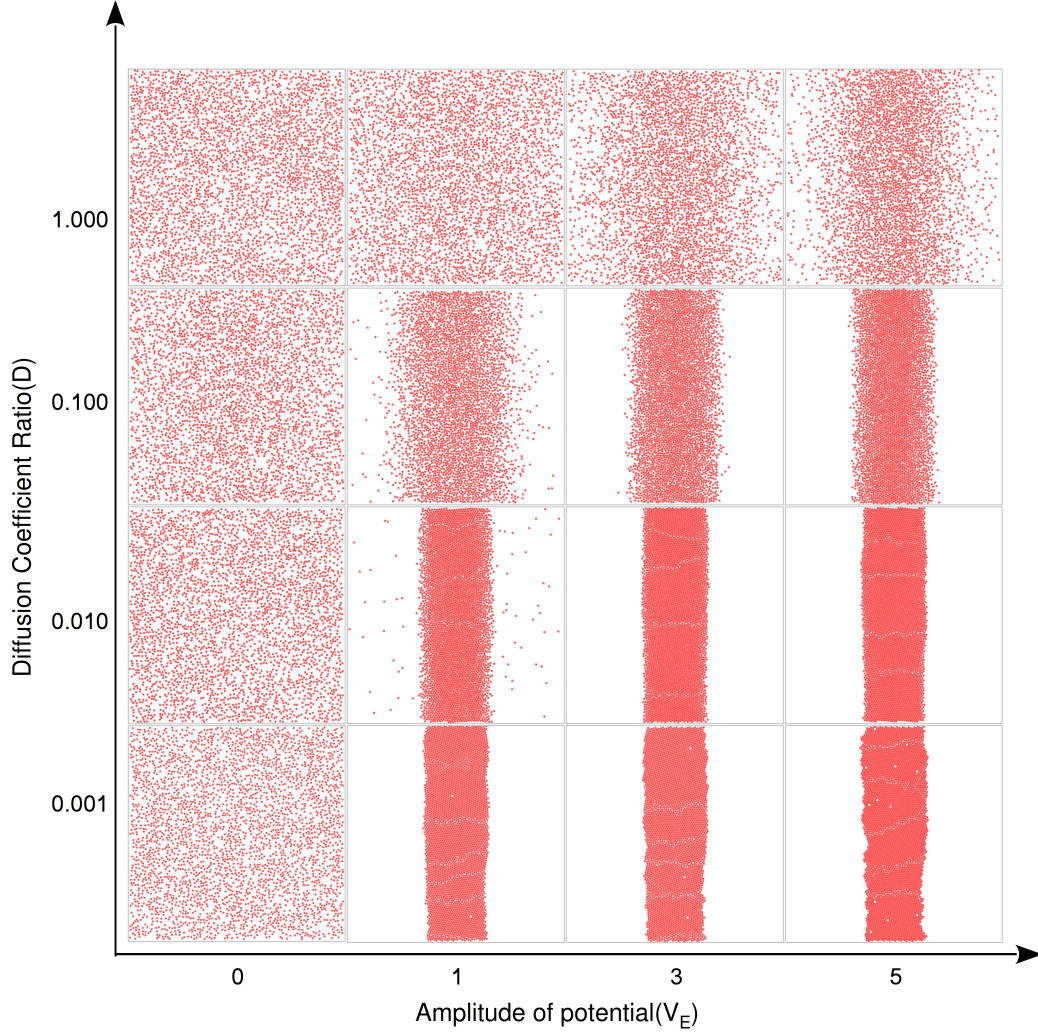


FIG. 1. Snapshots for single-component systems of particles with diffusion coefficient  $D_L$ , with  $N = N_L = 3184$  at  $t = 10^7$ , on a box of lateral dimension  $L_b = 200$ . The average density is  $\rho = 0.5$ . Different rows are for different values of  $D = D_L/D_H$  and different columns correspond to different values of the amplitude of the potential  $V_E$ . Note that, when changing  $D$ , we fixed the value of  $D_H$  and changed the value of  $D_L$ .

otherwise;  $r_{ij} = |\vec{r}_i - \vec{r}_j|$  is the distance between the particle centers and  $\hat{r}_{ij} = (\vec{r}_i - \vec{r}_j)/r_{ij}$ .  $\alpha \geq 0$  is the strength of repulsion.  $\mu$  is the inverse of the Stokes coefficient and it is the same for both species.  $\vec{\eta}_i$  is a Gaussian random white-noise term of zero mean ( $\langle \eta_i \rangle = 0$ ) and correlation  $\langle \eta_{in}(t)\eta_{jl}(t') \rangle = 2D_i\delta_{ij}\delta_{nl}\delta(t-t')$ , where  $D_i$  is the particle diffusion coefficient,  $\delta_{ij}$  and  $\delta_{nl}$  are Kronecker deltas, where  $n$  and  $l$  are the spatial components of the vectors  $\vec{\eta}_i$  and  $\vec{\eta}_j$ , respectively, and  $\delta(t-t')$  is the Dirac delta function. Note that, since  $\mu$  is the same for both species but  $D_i$  is not, the dynamics described by Eq. (1) does not obey the fluctuation dissipation theorem. In fact, the dynamics describes a mixture of passive particles at two distinct effective temperatures. The last term in Eq. (1) represents the interaction with the external potential. We consider,

$$V_{\text{ext}}(x) = V_E \cos(kx), \quad (2)$$

where  $V_E$  is the amplitude of the potential. We take  $k = \frac{2\pi}{L_b}$ , so that there is a single minimum at the center of the simulation box. Without loss of generality, we parameterize the system in terms of the ratio  $D = D_L/D_H$ , by fixing  $D_H$  and varying  $D_L$  and we define the density as  $\rho = N\pi a^2/L_b^2$ .

We performed simulations for square boxes of linear dimensions  $L_b = \{60, 80, 100, 120, 150, 200, 600, 1000\}$ , in units of the particle radius  $a$ , for  $\alpha = 90$  and  $\mu = 1$ . We integrated Eq. (1) using a second-order stochastic Runge-Kutta scheme [33], with a discrete time step  $dt = 2 \times 10^{-3}$ . Time is measured in units of  $a^2/D_H$ .

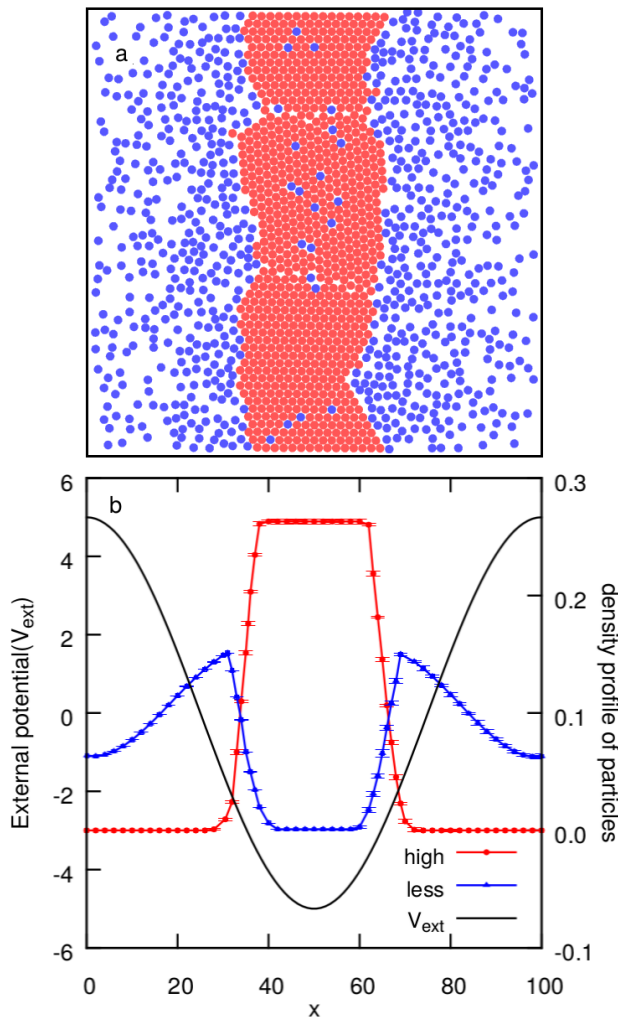


FIG. 2. (a) Snapshot and (b) density profile along the  $x$ -direction for a binary mixture of particles with low (red/light gray) and high (blue/dark gray) diffusion coefficients, for  $N_L = N_H = 796$ ,  $\rho = 0.5$ ,  $D = 10^{-3}$ , and  $V_E = 5$  at  $t = 10^7$ , in a box of lateral dimension  $L_b = 100$ . Each data point is an average over 25 samples. The error bars are smaller than the size of the symbols.

### III. RESULTS

Let us start by considering a single component system. Figure 1 depicts snapshots for different values of  $V_E$  and diffusion coefficient  $D_L$ , at a constant density  $\rho = 0.5$ , with initial uniform distribution. We use  $D = D_L/D_H$ , where  $D_H = 1$ , everywhere in this work. As shown in the figure, in the absence of the external potential ( $V_E = 0$ ), the particles are uniformly distributed, but for  $V_E \neq 0$ , the particles accumulate around the minimum of the potential (in the middle of the box) and a band is formed along the  $y$ -direction. The width of the band decreases as the amplitude of the external potential increases while it increases as the diffusion coefficient increases. These

results are in agreement with previous detailed studies of static and dynamical properties of single-component passive systems in the presence of similar external potentials [34].

We now consider equimolar binary mixtures ( $N_L = N_H = 796$ ), at the same total density  $\rho = 0.5$ , with a uniform initial distribution. Figure 2 depicts a snapshot (Fig. 2(a)) and the density profile (Fig. 2(b)) in the stationary state ( $t = 10^7$ ), for  $V_E = 5$  and  $D = 10^{-3}$ . The particles with low diffusion coefficients (red particles) tend to accumulate in the center of the band, in an ordered structure, surrounded by those with high diffusion coefficients (blue particles). Note that, for the given values of  $D_L$  and  $D_H$ , both species are expected to form a central band in the single-component system, as shown in Fig. 1, for  $D = 10^{-3}$  and  $D = 1$ , respectively.

In order to analyze the dependence of the dynamics on  $D$  and  $V_E$ , we illustrate in Fig. 3 snapshots of the stationary state at different values of these parameters. While in the absence of potential ( $V_E = 0$ ) demixing is observed only at low values of  $D$  ( $D < 0.1$ ), when the potential is switched on,  $V_E \neq 0$ , demixing occurs in the entire range of  $D$ , for strong enough  $V_E$ . In all cases, the particles with the low diffusion coefficient are those accumulating in the center of the band, forming a very compact cluster.

A more quantitative description of the demixing is obtained by calculating the number  $M$  of particles of the largest cluster of the species with the lower diffusion coefficient ( $D_L$ ). For the range of parameters where a band is formed in the center of the box, this cluster corresponds to the band itself. To identify the cluster, we used Voronoi tessellation [35]. We divided the space into  $N$  cells limited by polygons (one per particle), so that all the points in a cell are closer to the center of that particle than to the center of any other particle. Two particles are connected, if they are of the same species and the corresponding cells are first neighbors in the Voronoi tessellation. A cluster is then the set of all the connected particles.

Figure 4 illustrates the time evolution of the ratio  $M/N_L$ , for different values of the amplitude of the external potential  $V_E$ . The value of this ratio saturates asymptotically at a non-zero value that increases with  $V_E$ . This is consistent with demixing and cluster of particles with low diffusion coefficient, as shown in Fig. 3. Note that, for  $V_E = 0$  a non-zero value is also observed but in this case the largest cluster is not necessarily at the center of the box. The dependence of this ratio on  $D$  is plotted in Fig. 5, where different curves correspond to different values of  $V_E$ . The data points are extrapolations for the values in the thermodynamic limit, obtained from the dependence of this ratio on the box size, as shown in the inset. The lower the value of  $D$  the larger the fraction of particles in the largest cluster. In the limit of vanishing  $D$  (i.e.,  $D_L \ll D_H$ ), the ratio  $M/N_L$  converges to one. The threshold value of  $D$  below which demixing is observed is strongly affected by the value of  $V_E$ . In the



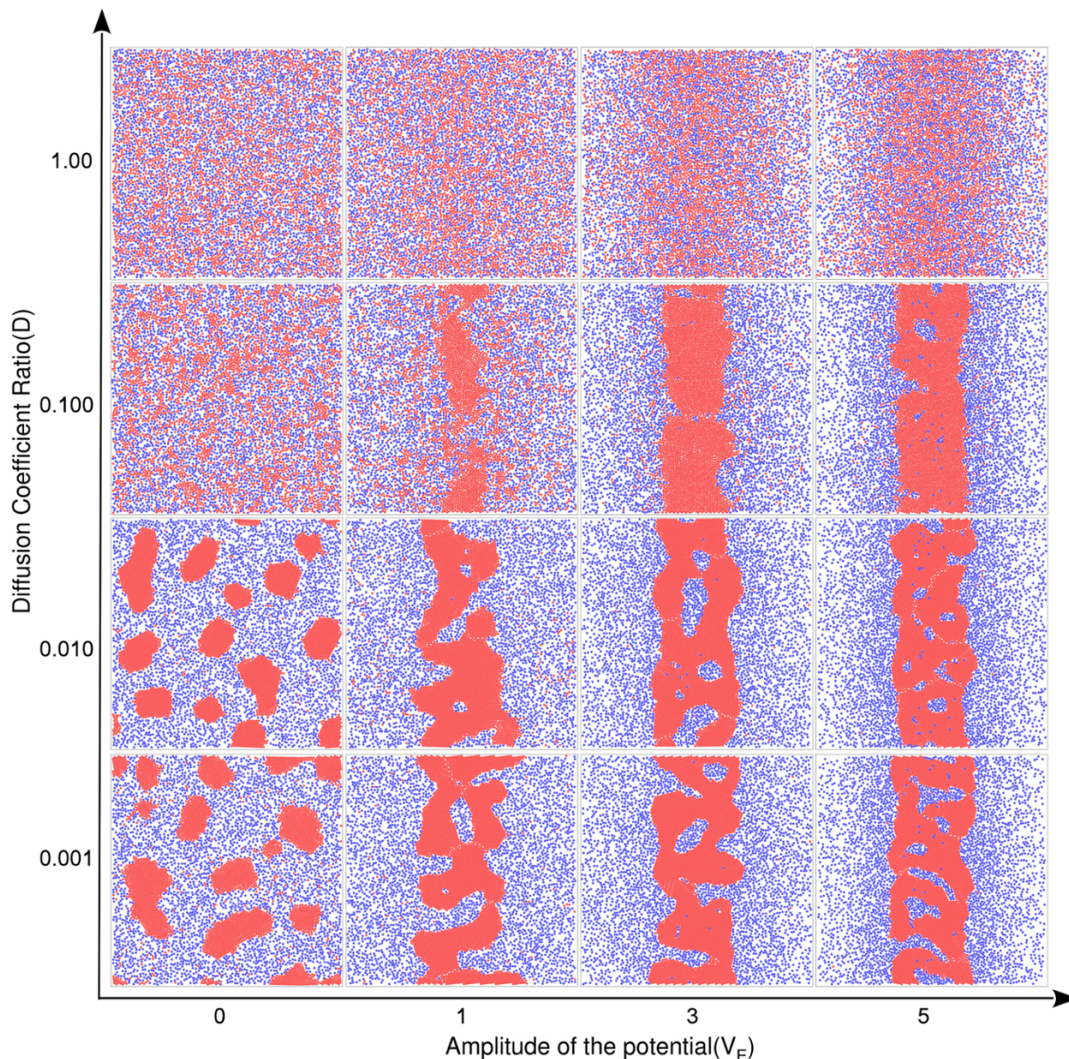


FIG. 3. Snapshots of binary mixtures, with  $N_L = N_H = 3184$  particles with low (red/light gray) and high (blue/dark gray) diffusion coefficients at  $t = 10^7$ , in a box of lateral dimension  $L_b = 200$ . The total density is  $\rho = 0.5$ . Different rows depict different values of  $D$  and different columns different values of the external potential amplitude  $V_E$ .

presence of a sinusoidal external potential, this threshold increases with  $V_E$ .

#### IV. FINAL REMARKS

We have shown, using Brownian dynamics simulations, that demixing of binary mixtures of particles with different effective diffusion coefficients is significantly enhanced in the presence of an external sinusoidal potential. For a one-dimensional spatially varying ( $x$ -dependent) potential with a minimum along the perpendicular ( $y$ -) direction, a band of particles with the lowest diffusion coefficient is formed along the minimum surrounded by particles with the highest diffusion coefficient. The stronger the external potential the smaller the difference required between the diffusion coefficients to observe demixing.

Electromagnetic fields, concentration gradients, and patterned substrates are examples of external stimuli that have been considered to control the dynamics of single-component active systems [31, 32, 36, 37]. Our results suggest that the dynamics of multicomponent systems is much richer than their single-component counterparts. In particular, demixing may occur and the conditions required are more general than in the absence of external stimuli. Future studies may consider the response to other external stimuli and how differences in the responsiveness of different species might affect the overall dynamics. Also, inspired by previous results for passive systems [38], it may be interesting to explore the emergence of new spatial-temporal patterns in the presence of time-varying stimuli.

## ACKNOWLEDGMENTS

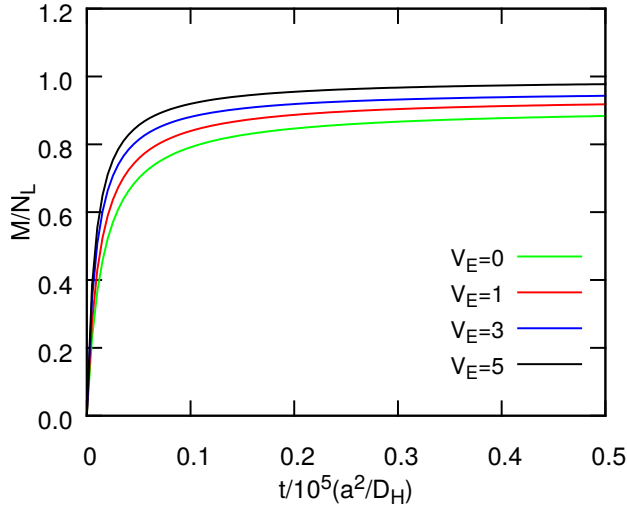


FIG. 4. Time dependence of the fraction of particles with low diffusion coefficient that belong to the largest cluster of this species,  $M/N_L$ , for different values of the amplitude of the external potential  $V_E$ , obtained from simulations of  $N = 1592$  particles in a box of lateral dimension  $L_b = 100$  ( $\rho = 0.5$ ) and  $D = 10^{-3}$ . Averages are over 25 samples.

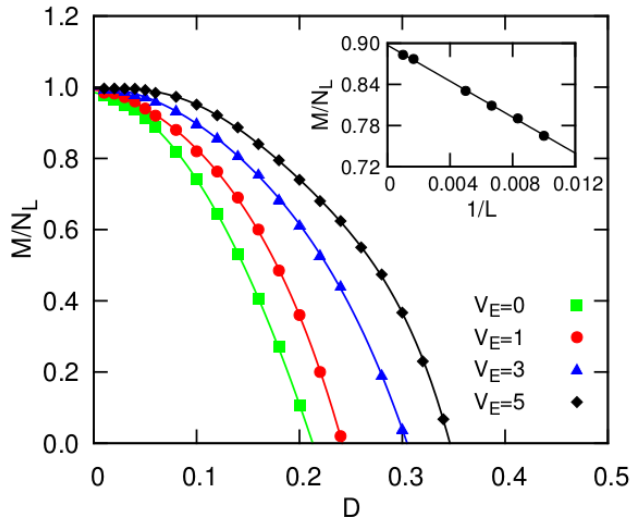


FIG. 5. Fraction of the particles with low diffusion coefficient that belong to the largest cluster of this species,  $M/N_L$ , as a function of the ratio  $D$ . Different symbols correspond to different values of the amplitude of the external potential  $V_E$ , at  $\rho = 0.5$ , obtained by extrapolating the dependence of  $M/N_L$  on the linear size of the box  $L_b$ ; boxes with  $L_b = \{100, 120, 150, 200, 600, 1000\}$  were considered. The inset shows an example, for  $V_E = 5$ , where the symbols represent the simulation data and the solid line is the linear fit.

We acknowledge financial support from the Portuguese Foundation for Science and Technology(FCT) under Contracts no UID/FIS/00618/2013 and SFRH/BD/119240/2016.

[1] K. Ahmad and I. J. Smalley, Powder Technol. **9**, 69 (1973).

[2] J. Dzubiella and H. Löwen, J. Phys. Condens. Matt **14**,

- 9383 (2002).
- [3] A. Kudrolli, Rep. Prog. Phys. **67**, 209 (2004).
  - [4] M. E. Leunissen, C. G. Christova, A. P. Hynninen, C. P. Royall, A. I. Campbell, A. Imhof, M. Dijkstra, R. van Roij, and A. van Blaaderen, Nature **437**, 235 (2005).
  - [5] G. C. M. A. Ehrhardt, A. Stephenson, and P. M. Reis, Phys. Rev. E. **71**, 041301 (2005).
  - [6] P. M. Reis, T. Sykes, and T. Mullin, Phys. Rev. E. **74**, 051306 (2006).
  - [7] T. Vissers, A. van Blaaderen, and A. Imhof, Phys. Rev. Lett. **106**, 228303 (2011).
  - [8] N. Rivas, P. Cordero, D. Risso, and R. Soto, New. J. Phys. **13**, 055018 (2011).
  - [9] N. Rivas, P. Cordero, D. Risso, and R. Soto, Granular Matter **14**, 157 (2012).
  - [10] M. Grünwald, S. Tricard, G. M. Whitesides, and P. L. Geissler, Soft Matter **12**, 1517 (2016).
  - [11] N. Rivas, S. Ponce, B. Gallet, D. Risso, R. Soto, P. Cordero, and N. Mujica, Phys. Rev. Lett. **106**, 088001 (2011).
  - [12] J. Stenhammar, R. Wittkowski, D. Marenduzzo, and M. E. Cates, Phys. Rev. Lett. **114**, 018301 (2015).
  - [13] S. N. Weber, C. A. Weber, and E. Frey, Phys. Rev. Lett. **116**, 058301 (2016).
  - [14] S. Ramaswamy, Annu. Rev. Condens. Matt. Phys. **1**, 323 (2010).
  - [15] C. Bechinger, R. D. Leonardo, H. Löwen, C. Reichhardt, G. Volpe, and G. Volpe, Rev. Mod. Phys. **88**, 045006 (2016).
  - [16] X. Trepát, M. R. Wasserman, T. E. Angelini, D. A. W. E. Millet, J. P. Butler, and J. J. Fredberg, Nature Physics **5**, 426 (2009).
  - [17] T. E. Angelini, E. Hannezo, X. Trepát, M. Marquez, J. J. Fredberg, and D. A. Weitz, PNAS **108**, 4714 (2011).
  - [18] L. Chai, H. Vlamakis, and R. Kolter, MRS Bulletin **36**, 374 (2011).
  - [19] K. Drescher, J. Dunkel, L. H. Cisneros, S. Ganguly, and R. E. Goldstein, PNAS **108**, 10940 (2011).
  - [20] R. Ni, M. A. C. Stuart, M. Dijkstra, and P. G. Bolhuis, Soft Matter **10**, 6609 (2014).
  - [21] F. Kummel, P. Shabestari, C. Lozano, G. Volpe, and C. Bechinger, Soft Matter **11**, 6187 (2015).
  - [22] S. C. Takatori and J. F. Brady, Soft Matter **11**, 7920 (2015).
  - [23] J. Smrek and K. Kremer, Phys. Rev. Lett. **118**, 098002 (2017).
  - [24] X. Yang, M. L. Manning, and M. C. Marchetti, Soft Matter **10**, 6477 (2014).
  - [25] A. Y. Grosberg and J. F. Joanny, Phys. Rev. E. **92**, 032118 (2015).
  - [26] H. Tanaka, A. A. Lee, and M. P. Brenner, Phys. Rev. Fluids **2**, 043103 (2017).
  - [27] J. Adler, Science **153**, 708 (1966).
  - [28] J. P. Armitage and K. J. Hellingwerf, Photosynth. Res **76**, 145 (2003).
  - [29] R. Blakemore, Science **190**, 377 (1975).
  - [30] A. Bricard, J. B. Caussin, N. Desreumaux, O. Dauchot, and D. Bartolo, Nature **503**, 95 (2013).
  - [31] J. Yan, M. Han, J. Zhang, C. Xu, E. Lujiten, and S. Granick, Nature Materials **15**, 1095 (2016).
  - [32] A. Boymelgreen, G. Yossifon, and T. Miloh, Langmuir **32**, 9540 (2016).
  - [33] A. C. Branka and D. M. Heyes, Phys. Rev. E **60**, 2381 (1999).
  - [34] A. S. Nunes, N. A. M. Araujo, and M. M. T. da. Gama, J. Chem. Phys. **44**, 034902 (2016).
  - [35] S. Fortune, Algorithmica **2**, 153 (1987).
  - [36] E. Pinçe, S. K. P. Velu, A. Callegari, P. Elahi, S. Gigan, G. Volpe, and G. Volpe, Nat. Comm. **7**, 10907 (2016).
  - [37] D. McDermott, C. J. O. Reichhardt, and C. Reichhardt, Soft Matter **12**, 8606 (2016).
  - [38] N. A. M. Araújo, D. A. Zezyulin, V. V. Konotop, and M. M. T. da Gama, “Dynamical design of spatial patterns of colloidal suspensions,” arXiv:1706.02067.